MIMO Robust Control for HVAC Systems

Michael Anderson, Michael Buehner, *Student Member, IEEE*, Peter Young, *Member, IEEE*, Douglas Hittle, Charles Anderson, Jilin Tu, and David Hodgson

***Abstract*—Potential improvements in heating, ventilating, and air conditioning (HVAC) system performance are investigated through the application of multiple-input–multiple-output (MIMO) robust controllers. This approach differs dramatically from today's prevalent method of building HVAC controllers using multiple single-input–single-output control loops. A simulation model of an experimental HVAC system is used in the design and simulation testing of controllers. While simulation can be insightful, the only way to truly verify the performance provided by different HVAC controller designs is by actually using them to control an HVAC system. Thus, an experimental HVAC system was built for testing a wide range of advanced HVAC controllers. The design and testing of MIMO robust controllers provides valuable insight into potential improvements in performance, as well as constraints, associated with applying this control methodology to HVAC systems. Test results on the physical system demonstrate achievable performance gains (reductions in discharge air temperature settle time) in excess of 300%. Furthermore, these performance gains may be achieved without significant impact to current HVAC system architecture (interconnection).**

***Index Terms*—Discharge air system, experimental verification, heating, ventilating, and air conditioning (HVAC), MATLAB, multiple-input–multiple-output (MIMO) robust $\mathcal{H}_\infty$ control, Realtime Workshop (RTW), Simulink, Windows Target.**

I. Introduction

IN COMMERCIAL heating, ventilating, and air conditioning (HVAC) systems, a *central air supply* provides air at a controlled temperature and flow rate for use in heating (or cooling) a space. A heating coil is used in the central air supply for heating the discharged air. The temperature of the discharged air is controlled by regulating the rate at which hot water flows through the heating coil. The flow rate of the discharged air is regulated to maintain a predetermined static air pressure within the temperature controlled space. Typically, the space within a building is divided into smaller *zones*, allowing the temperature within each zone to be maintained independently of the others. Each zone contains a reheat coil which is used to moderate the final temperature of the air discharged into the zone.

Manuscript received November 9, 2006. Manuscript received in final form April 20, 2007. Recommended by Associate Editor B. de Jagar. This work was supported by the National Science Foundation under Award 9804757, Award 9732986, and Award 0245291.

M. Anderson, M. Buehner, and P. Young are with the Department of Electrical and Computer Engineering, Colorado State University, Fort Collins, CO 80523 USA (e-mail: mlanderson@hotmail.com; mbuehner@engr.colostate.edu; pmy@engr.colostate.edu).

D. Hittle and D. Hodgson are are with the Department of Mechanical Engineering, Colorado State University, Fort Collins, CO 80523 USA (e-mail: hittle@lamar.colostate.edu; dh688526@engr.colostate.edu).

C. Anderson and J. Tu are with the Department of Computer Science, Colorado State University, Fort Collins, CO 80523 USA (e-mail: anderson@cs.colostate.edu; jlintu@ifp.uiuc.edu).

Digital Object Identifier 10.1109/TCST.2007.903392

Early investigations into HVAC control focused on distributed system-input–system-output (SISO) proportional–integral (PI) controllers. It has long been recognized that the necessarily low gains and tedious and (sometimes) inaccurate tuning of PI-based HVAC controllers contributed to poor performance [9], [11]. Also, SISO controllers are unable to take advantage of the multivariable interactions in an HVAC system, which makes multiple-input–multiple-output (MIMO) controllers more attractive. To this extent, optimal control has been proposed as a means for MIMO-based controller design (e.g., [7], [16], [17]); however, an optimal controller's sensitivity to discrepancies between the model used in designing the controller and that of the physical plant (model uncertainty) poses a major problem in HVAC systems, where accurate models are not readily available. Furthermore, the characteristics of an HVAC plant change (deteriorate) over time. Nonetheless, several optimal HVAC controller designs have been simulated and one has been tested on a simple system [7].

The application of *robust control* theory in controlling HVAC systems has only recently been considered. It has been proposed as a means to account for and compensate for both the uncertainty associated with the model used in controller design and the nonlinear nature of HVAC systems [4]. SISO robust controllers have been implemented and their performance verified in simulation [13] and on an experimental HVAC system [8]. The utilization of robust control techniques has also seen some application on a two-input–two-output room sized air conditioner [5] and regulating airflow for ventilation [14]. The work presented here is on the design and implementation of multivariable robust controllers for commercial style HVAC systems.

In Section II, the physical system used to test the controller is described. Sections III–VIII discuss the design and implementation of a MIMO robust controller for a HVAC application. Section IX shows how the designed weight may be used to easily explore various controller architectures and Section X compares the results of the various controllers on the physical HVAC system.

II. Experimental HVAC System

The experimental HVAC system shown in Fig. 1 was constructed for verifying the performance of the advanced HVAC controller designs. This system consisted of external and return air dampers, a variable speed blower, and a heating coil, which are similar to commercial hot water-to-air heating systems. A diagram representing this system is shown in Fig. 2 with the mnemonics defined in Table I.

The temperature of the discharged air was a function of the temperature and flow rate of both the air and water flowing through the coil. The flow rate of the air was primarily a function of the speed at which the blower is operating, but was affected slightly by the position of the return and external dampers. The

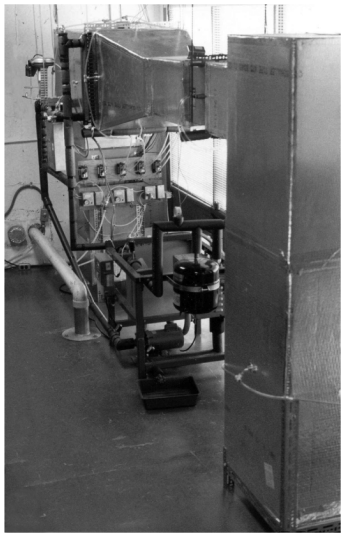

Fig. 1. The experimental HVAC system.

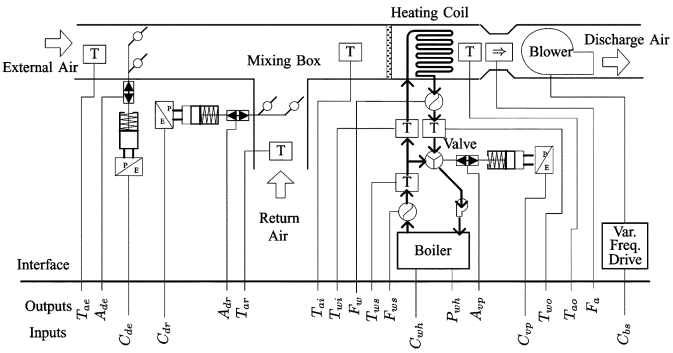

Fig. 2. Diagram of the experimental system and interface signals.

TABLE I
KEY TO MNEMONICS

C_{dr}	Command damper return	T_{ai}	Temp. of air input
C_{de}	Command damper external	T_{ao}	Temp. of air output
C_{wh}	Command water heater	T_{ws}	Temp. of water supply
C_{vp}	Command valve position	T_{wi}	Temp. of water into coil
C_{bs}	Command blower speed	T_{wo}	Temp. of water out of coil
		T_{ae}	Temp. of air external
A_{dr}	Actual damper return	T_{ar}	Temp. of air return
A_{de}	Actual damper external	F_w	Flow rate of water (coil)
A_{vp}	Actual valve position	F_{ws}	Flow rate of water (system)
P_{wh}	Power (input) water heater	F_a	Flow rate of air

dampers were electronically "ganged" together, allowing the return and external (outside) air mix to be varied, in regulating the temperature of the air flowing into the coil. A three-way mixing valve allows the flow rate of the water through the coil to be varied.

Controllers for the experimental system were implemented using MATLAB and *Simulink* with the *Real-Time Workshop* (RTW) and *Windows Target* toolboxes on a *Windows98*-based PC fitted with standard data acquisition cards. The design, construction, commissioning, and modelling of this system is covered in previous works [1], [2].

III. MIMO ROBUST CONTROL SYNTHESIS

Inevitably, the models used in controller design only approximate the physical systems they intend to represent. *Robust control* theory addresses the affects that discrepancies between the model and the physical system (model uncertainty) may have on the design and performance of (linear) feedback systems. These uncertainties may arise from model approximation, neglected or unmodeled dynamics, unknown parameters, or even sensor and/or actuator imperfections. The techniques for dealing with model uncertainty used here are based upon the structured singular value (μ) [10]. Robust control provides a unified design approach under which the concepts of gain margin, phase margin, tracking, disturbance rejection, and noise rejection are generalized into a single framework. Typically, the uncertainties considered in robust control theory are bounded using norms. The $\mathcal{H}_\infty$ and $\mathcal{H}_2$ norms are frequently applied in the robust controller design process [12]. Herein, only the $\mathcal{H}_\infty$ robust control design methodology is considered.

It should be noted that μ-synthesis is *not* the only way to synthesize a robust controller, but it is the method chosen for this application. In this brief, the task of controller design was carried out using the MATLAB *μ-Analysis and Synthesis Tool Box* [3]. For more information regarding robust control theory see [10], [12], and [15].

IV. MIMO ROBUST HVAC CONTROLLER DESIGN

To simplify the formulation, controller designs for the experimental HVAC system were restricted to *discharge air temperature and airflow rate control* (i.e., command T_{ao} and F_a to track reference inputs). The resulting *discharge air system* (DAS) is similar to the central air supply in a commercial HVAC system.

The four key control variables in a DAS are the input air and water temperatures (T_{ai} and T_{wi}) and flow rates (F_a and F_w) supplied to the heating coil. In current HVAC systems, a common water supply typically provides hot water to multiple heating coils (i.e., T_{wi} is held constant). Thus, the water supply temperature cannot be varied at each DAS.

The design of an $\mathcal{H}_\infty$ robust controller involves selecting frequency dependent weighting functions (transfer functions) that define the model uncertainty and the $\mathcal{H}_\infty$ optimization criteria. To facilitate the design of these weighting functions, the experimental system model was arranged in a *canonical form* for controller synthesis, which is shown in Fig. 3. This canonical form isolates the exogenous inputs (w_1 and w_2) and exogenous outputs (z_1 and z_2). The exogenous inputs are the weighted external disturbances and commanded inputs (w_1) and the weighted sensor noise measurements (w_2), an inevitable component of measurement signals. The exogenous outputs are the weighted error signals to be minimized (z_1) and the weighted controller outputs (z_2). Equation (1) shows the signals (used in the design of the robust controller in

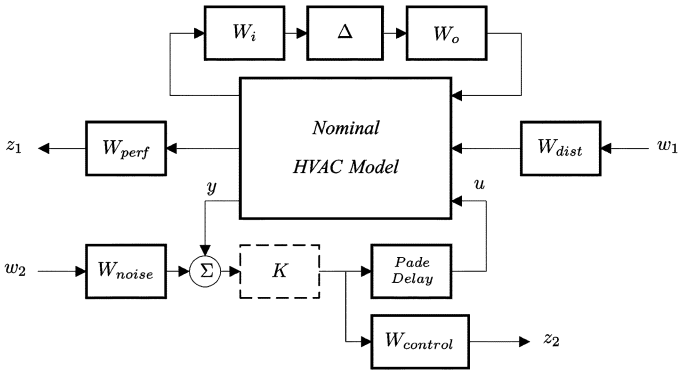

Fig. 3. System model configuration for controller synthesis.

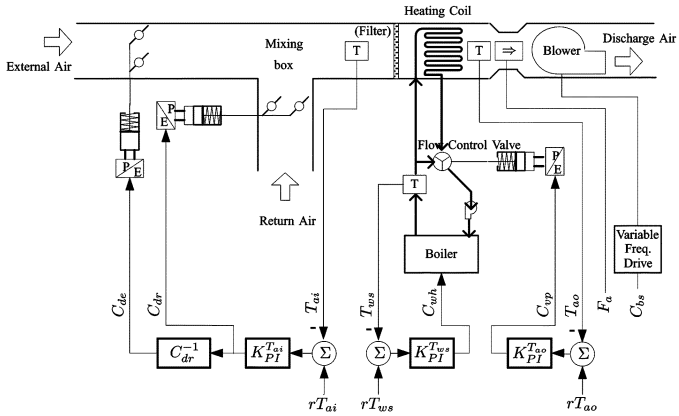

Fig. 4. HVAC controller based on three SISO PI controllers.

Section VII) associated with the vectors w_1, w_2, z_1, z_2, u, and y.

$$w_1 = \begin{bmatrix} T_{ae} \\ T_{ar} \\ \Delta F_a \\ rF_a \\ rT_{ao} \\ rT_{ws} \\ rT_{ai} \end{bmatrix} \quad z_1 = \begin{bmatrix} errorF_a \\ errorT_{ai} \\ errorT_{ws} \\ errorT_{ao} \end{bmatrix} \quad u = \begin{bmatrix} C_{vp} \\ C_{bs} \\ C_{dr} \\ C_{wh} \end{bmatrix}$$

$$w_2 = \begin{bmatrix} noiseF_w \\ noiseF_a \\ noiseT_{ai} \\ noiseT_{ws} \\ noiseT_{wi} \\ noiseT_{wo} \\ noiseT_{ao} \\ noiseT_{ae} \\ noiseT_{ar} \end{bmatrix} \quad z_2 = \begin{bmatrix} C_{vp} \\ C_{bs} \\ C_{dr} \\ C_{wh} \end{bmatrix} \quad y = \begin{bmatrix} F_w \\ errorF_a \\ errorT_{ai} \\ errorT_{ws} \\ T_{wi} \\ T_{wo} \\ errorT_{ao} \end{bmatrix} \tag{1}$$

Note: vectors w_1, w_2, z_1, and z_2 are weighted (optimization criteria), vectors u and y are not weighted (physical signals).

As the structure of the controller is embedded in the nominal plant model, many controller architectures may be realized using the generalized model shown in Fig. 3. The signals comprising the vectors w_1, w_2, z_1, z_2, u, and y depend upon this structure. As the design is performed in continuous-time and the controller implemented in discrete-time, *Pade* delays are used in the feedback loop to include the effects of sampling.

V. Overview of HVAC Controller Designs

For reference, a distributed PI-based controller was constructed. This reference PI controller was designed using the techniques from [6] to optimize the closed-loop performance on the physical system. While a PI controller would be rarely be tuned this well to a physical system, much effort was put into fine tuning this controller in order to demonstrate that a MIMO controller can outperform even the best SISO-based PI controller. A block diagram of the SISO-based PI controller is given in Fig. 4.

The MIMO robust controller K_{R2} (which is labelled as such to be consistent with [1]) was designed as a seven-input–four-output controller. The seven inputs consisted of the regulated outputs F_a, T_{ai}, T_{ao}, T_{ws}, and measurements that affected the regulated outputs, namely F_w, T_{wi}, and T_{wo}. The four controller outputs were the commanded outputs C_{dr}, C_{wh}, C_{vp}, and C_{bs}. A block diagram of controller K_{R2} is shown Fig. 5. Note that since the dampers were ganged together, only one control signal, namely C_{dr}, was required (i.e., C_{de} was determined from C_{dr}). For more information on the model, see [1], [2].

In Sections VI and VII, the design of the reference PI controller and the K_{R2} MIMO robust controllers will be discussed in detail. A similar design procedure may be used for designing the other MIMO robust controllers. Examples of these controllers will be discussed at the end of this paper.

VI. Reference PI Controller Design

Contemporary HVAC controllers utilize multiple PI controllers to regulate individual SISO control loops. Since the blower fan already had a built-in controller (variable frequency drive), the airflow rate (F_a) was controlled by commanded blower speed (C_{bs}). Therefore, only three (SISO) PI controllers, namely $K_{PI}^{T_{ws}}$, $K_{PI}^{T_{ai}}$, and $K_{PI}^{T_{ao}}$, were used to control the commanded water heater temperature (C_{wh}), commanded return (and hence external) air damper position (C_{dr} and hence C_{de}), and commanded valve position (C_{vp}), respectively. This is illustrated in Fig. 4.

Though providing tolerable performance, the PI control faces several challenges. First, the subsystems that they control have gains that vary nonlinearly. Thus, the PI controller must be tuned at the highest gain state to maintain stability over the entire range. This provides a slow response in low gain states. This makes tuning the PI controller time consuming and tedious, with optimal performance rarely attained. Nonetheless, considerable effort was put into the design of these controllers to get the best possible response on the physical system. Specifically, these gains were tuned for the experimental HVAC system using the method outlined in [6, p. 285]. The final controller gains are given in Table II.

Windup is another problem common in HVAC systems, which occurs when the controller states become inconsistent with the control signals (e.g., a linear control drives an actuator into saturation). Following such an occurrence, the control loop may experience severe transients. The PI controller design

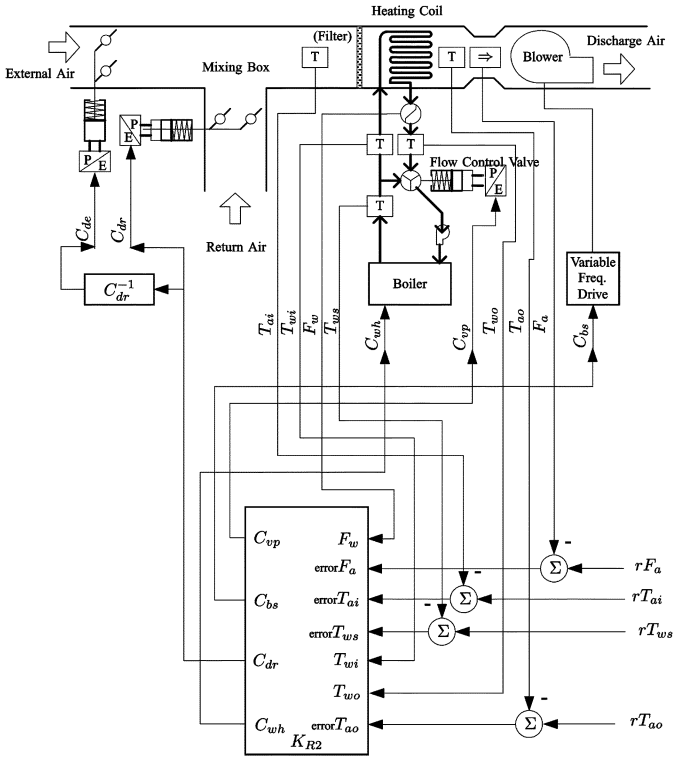

Fig. 5. Experimental system using MIMO robust controller K_{R2}.

TABLE II
PROPORTIONAL AND INTEGRAL GAINS FOR PI CONTROLLERS

PI Controller	Proportional Gain(K_p)	Integral Gain(K_i)
(K_{PI}^{Tai})	0.20	0.010
(K_{PI}^{Tao})	0.24	0.025
(K_{PI}^{Tws})	1.80	0.015

presented herein employed an antiwindup technique to avoid this problem.

VII. MIMO ROBUST CONTROLLER K_{R2} DESIGN

The first step in designing the K_{R2} controller was to determine the system and controller architectures. Controller K_{R2} controlled the water supply temperature (T_{ws}), input air temperature (T_{ai}), air flow rate (F_a), and the discharge air temperature (T_{ao}). A system interconnect incorporating this controller is shown in Fig. 5.

The K_{R2} controller synthesis task required a more detailed description than the canonical synthesis model shown in Fig. 3. This was accomplished by creating a textual description (defined using *sysic*, a component of the MATLAB *μ-Analysis and Synthesis Toolbox*) of the model (given in [1]) that defined the overall HVAC system interconnect and associated weighting functions. The crux of the design is to select the frequency dependent weights, which are discussed in detail in Sections VII-A and VII-B.

A. Model Uncertainty Weight Selection

Additive uncertainty was incorporated around each of the five subsystems (see Table III). For each subsystem, the number of additive uncertainty weights was determined by the number of physical inputs and outputs. The number of inputs and outputs for each subsystems determined the size of individual blocks in $\Delta = \mathrm{diag}(\Delta_V, \Delta_B, \Delta_M, \Delta_H, \Delta_C)$. Note that each subsystem had its own uncertainty block.

TABLE III
MODEL UNCERTAINTY WEIGHTS USED IN THE DESIGN OF K_{R2}

Valve Uncertainty					
$w_{V_{in}}(C_{vp})$	=	0.001	$w_{V_{out}}(F_w)$	=	0.005
			$w_{V_{out}}(F_{ws})$	=	0.005
Blower Uncertainty					
$w_{B_{in}}(C_{bs})$	=	0.001	$w_{B_{out}}(F_a)$	=	0.005
$w_{B_{in}}(C_{dr})$	=	0.001			
Mixing Box Uncertainty					
$w_{M_{in}}(C_{dr})$	=	0.005			
$w_{M_{in}}(T_{ar})$	=	0.005	$w_{M_{out}}(T_{ai})$	=	0.001
$w_{M_{in}}(T_{ae})$	=	0.005			
Water Heater (Boiler) Uncertainty					
$w_{H_{in}}(C_{wh})$	=	0.005			
$w_{H_{in}}(T_{wo})$	=	0.005	$w_{H_{out}}(T_{ws})$	=	0.001
$w_{H_{in}}(F_w)$	=	0.005			
$w_{H_{in}}(F_{ws})$	=	0.005			
Heating Coil Uncertainty					
$w_{C_{in}}(F_a)$	=	0.005			
$w_{C_{in}}(F_w)$	=	0.005	$w_{C_{out}}(T_{wo})$	=	0.001
$w_{C_{in}}(T_{ai})$	=	0.005	$w_{C_{out}}(T_{ao})$	=	0.001
$w_{C_{in}}(T_{wi})$	=	0.005			

The model uncertainty for each subsystem was split into uncertainty on the inputs (W_i) and uncertainty on the outputs (W_o). While it is possible to lump all of the uncertainty into either the input or the output, splitting up the uncertainty description will give a more balanced H_∞ design.

The amount of model uncertainty used did not have a large impact on the performance of the synthesized controller in simulation. Therefore, constant model uncertainty weights were used that were based on the quality of fit from the modeling phase [2]. Since the overall uncertainty for a subsystem is (effectively) determined by the product of the input and output weights, each of the five subsystems had the same effective uncertainty description. The weights for each subsystem are summarized in Table III.

B. Optimization Criteria Weight Selection

The optimization criteria weights were used to scale the normalized inputs and outputs to represent the relative magnitudes seen by the physical HVAC system. When a weight was too small, the $\mathcal{H}_\infty$ controller synthesis software assumed that the signal would not have a large enough magnitude to affect the overall stability. This often resulted in a controller that was over-reactive (e.g., if too much control authority is given to a particular control signal). Similarly, when a weight was too large, the $\mathcal{H}_\infty$ controller synthesis software put too much effort into minimizing the gain of a signal that the physical system would never see. This usually lead to a lack of performance. Ultimately, the magnitudes and frequency ranges of the weights had to be tuned until the fastest response (while maintaining disturbance rejection) was obtained in simulation.

TABLE IV
DISTURBANCE (AND REFERENCE) WEIGHTS USED IN THE DESIGN OF K_{R2}

$w_{Dist}(T_{ae})$	=	$\frac{0.01}{s+0.02}$	$w_{Dist}(T_{ar})$	=	$\frac{0.01}{s+0.02}$
$w_{Dist}(\Delta F_a)$	=	$\frac{0.01}{s+2}$	$w_{Dist}(rF_a)$	=	$\frac{0.8}{s+1}$
$w_{Dist}(rT_{ao})$	=	$\frac{5}{s+1}$	$w_{Dist}(rT_{ws})$	=	$\frac{1}{s+1}$
$w_{Dist}(rT_{ai})$	=	$\frac{1}{s+1}$			

TABLE V
PERFORMANCE WEIGHTS USED IN THE DESIGN OF K_{R2}

$w_{Perf}(F_a)$	=	$\frac{0.1}{s+0.0002}$	$w_{Perf}(T_{ao})$	=	$\frac{0.005}{s+0.00025}$
$w_{Perf}(T_{ai})$	=	$\frac{0.001}{s+5\times10^{-5}}$	$w_{Perf}(T_{ws})$	=	$\frac{0.02}{s+0.004}$

1) Disturbance Weights: For the K_{R2} controller, the disturbances (w_1) consisted of air temperatures from the surrounding environment (T_{ae} and T_{ar}), variations in the flow rate of air (ΔF_a) due to wind gusts and commanded inputs (rT_{ao}, rF_a, rT_{ai}, and rT_{ws}). The air temperatures from the environment generally did not change vary rapidly, so the disturbance weights associated with them had a bandwidth of 3 mHz. Since these disturbances did not affect the output as much as the reference inputs, a gain of 0.5 was used. The wind gusts were assumed to have an even smaller affect on the outputs, so its magnitude was 0.005 in the passband. This weight covered wind gusts in the dc to 0.32 Hz (2 rad/s) range, which was enough bandwidth to "cover" the wind gusts seen in experimental testing. The reference input weights all had a cutoff frequency of 0.16 Hz (1 rad/s), which was reasonable since the highest frequency allowed for controlling the valve and the dampers was about 0.1 Hz (see Section VII-B4 on control weight selection). Since the reference signals were the largest disturbance signals, they had the largest passband magnitudes. The transfer functions used to describe these weights are given in Table IV.

2) Performance Weights: The performance weights were chosen to specify the performance objectives that the controller was to attain. In particular, good steady-state tracking was desired, so these weights had large values at dc and then rolled off above 0.1 mHz. A particular design choice for this controller was to make the input air temperature weight only focused on steady-state values. This allowed for the input air to vary as the output air set point was being tracked. The result of this is evident in the test results of the controller on the physical system. NB: If this feature were to be eliminated, then the low pass pole in the weight $w_{\mathrm{Perf}}(T_{ai})$ could be pushed out to a higher frequency. The transfer functions describing these weights are given in Table V.

3) Sensor Noise Weights: Sensor noise is typically a high frequency phenomenon (i.e., sensors are assumed to be most accurate at frequencies around dc). Therefore, these weights were chosen to be HPFs. When possible, these weights are chosen based on the sensor product description. While these weights generally do not have a large impact on the synthesized controller, they play an important role, namely they guarantee that the $\mathcal{H}_\infty$ optimization is well posed [12]. The transfer functions describing the sensor noise weights are given in Table VI.

TABLE VI
SENSOR NOISE WEIGHTS USED IN THE DESIGN OF K_{R2}

$w_{SN}(F_w)$	=	$\frac{10s+1\times10^{-6}}{1\times10^{6}s+1}$	$w_{SN}(F_a)$	=	$\frac{0.1s+0.001}{0.1429s+1}$
$w_{SN}(T_{ai})$	=	$\frac{0.1s+0.001}{0.1s+1}$	$w_{SN}(T_{ws})$	=	$\frac{0.05s+0.01}{0.05s+1}$
$w_{SN}(T_{wi})$	=	$\frac{0.05s+0.01}{0.05s+1}$	$w_{SN}(T_{wo})$	=	$\frac{0.05s+0.01}{0.05s+1}$
$w_{SN}(T_{ao})$	=	$\frac{0.1s+0.01}{0.1s+1}$	$w_{SN}(T_{ae})$	=	$\frac{0.1s+0.01}{0.1s+1}$
$w_{SN}(T_{ar})$	=	$\frac{0.1s+0.01}{0.1s+1}$			

TABLE VII
CONTROL WEIGHTS USED IN THE DESIGN OF K_{R2}

$w_{Cont}(C_{vp})$	=	$\frac{2s+0.015}{0.2s+1}$	$w_{Cont}(C_{bs})$	=	$\frac{0.1592s+0.01}{0.01592s+1}$
$w_{Cont}(C_{wh})$	=	$\frac{0.1592s+0.15}{0.001592s+1}$	$w_{Cont}(C_{dr})$	=	$\frac{1.333s+0.02}{0.1333s+1}$

4) Control Weights: The control weights had the most impact on the synthesized controller. The flow control value and the dampers were pneumatically controlled, which resulted in them responding the slowest to step changes. Therefore, their control inputs (C_{vp} and C_{dr}) were allowed to provide large control signals in the dc to 2-mHz range and were forced to be negligible above the 1-Hz range. The blower had a built-in controller that was able to change the flow rate of air (F_a) with the commanded blower speed (C_{bs}); however, high frequency changes in one variable disrupted the other outputs. Therefore, the commanded blower speed (C_{bs}) was allowed to have the largest control signals in the dc to 10-mHz range, and was forced to be negligible above 10 Hz. For the three weights discussed so far, the control weights were in the 0.01–0.02 magnitude range. For this system, weight values below 0.01 resulted in overactive controllers and weight values above 0.02 resulted in a controller that had a longer settling time. The fourth control variable was the commanded water temperature in the system (C_{wh}). The water heater required smaller control signals, so a larger weight (about ten times the size of the blower speed weight was used. Both the blower speed weight and the water heater weight reached a magnitude of one around the 1-Hz range, which may be viewed as a loose upper bound to the fastest controllable dynamic in the HVAC system. The transfer functions describing the control weights are given in Table VII.

C. Controller Implementation

Three $D-K$ iterations were performed to synthesize the MIMO robust controller K_{R2}, which resulted in a 58th-order controller. After model reduction was performed, the controller was reduced to a 22nd-order controller. The resulting continuous-time state-space controller was converted to a digital

state-space controller using a zeroth-order hold transformation. Since speed is not generally an issue in HVAC systems, the 22nd-order controller was easily implemented on the physical system, which ran at a 10-Hz sampling rate. Furthermore, the controller's system poles were made up of 8 real poles and 14 complex poles, which means that a similarity transformation could be performed on the state matrix to diagonalize it, where two-by-two blocks would be used for the complex eigenvalues in the state matrix. This reduce the number of multiply and accumulates from 484 (for the full 22-by-22 state matrix) to 36 (for the diagonalized matrix) for each (state) matrix product, which could easily be handled by current digital signal processors.

VIII. Experimental Verification of Controllers

The two criteria of tracking step changes and disturbance rejection were used to evaluate the controllers. Large step changes could occur in the morning when the whole building is being brought to a comfortable temperature and right before a meeting is scheduled to occur in a sectioned off room (e.g., a conference room). While the second situation is not currently used since a large step change may take up to 15 min, it would be more practical with a MIMO controller that can reach a set point in 1.5–3 min. This type of flexibility would help conserve energy in a building. As for disturbance rejection, this is required to keep temperature constant as larger quantities of people move from zone-to-zone. In Section VIII-A and VIII-B, the results from running experiments on a physical system with distributed PI controllers and a MIMO controller are examined. The results demonstrate that a commercial style HVAC system is truly a multivariable plant that can benefit greatly from a multivariable controller.

A. Reference PI Controller Verification

A Simulink model in conjunction with MATLAB's *Real-Time Workshop Toolbox* (RTW) was used to test the performance of the reference PI controller. In order to get a good controller on the physical system, the iterative process of redesigning and retesting was performed. After the experimental system was running and had reached steady state under closed-loop control, it was subjected to a series of step changes in the output air temperature (rT_{ao}) and air flow rate (rF_a) reference inputs. The response of the experimental system to these inputs is shown in Fig. 6.

For an example step change, the output air temperature reference (rT_{ao}) was increased (stepped) from 39.5 °C to 44.5 °C, which occurred around second 300. The controller $K_{PI}^{T_{ao}}$ responded by increasing the valve position (C_{vp}) output [increasing the water flow rate (F_w)], which caused the temperature of the discharge air (T_{ao}) to rise. After 931 s elapsed, the reference level was reached.

For an example of disturbance rejection, the air flow rate (rF_a using the C_{bs} output) was abruptly stepped down (around second 1800) from 0.272 m^3/s (38.2% of the maximum rate) to 0.151 m^3/s (21.4%). In response to the rising temperature of the output air (T_{ao}), the controller $K_{PI}^{T_{ao}}$ reduced the valve position

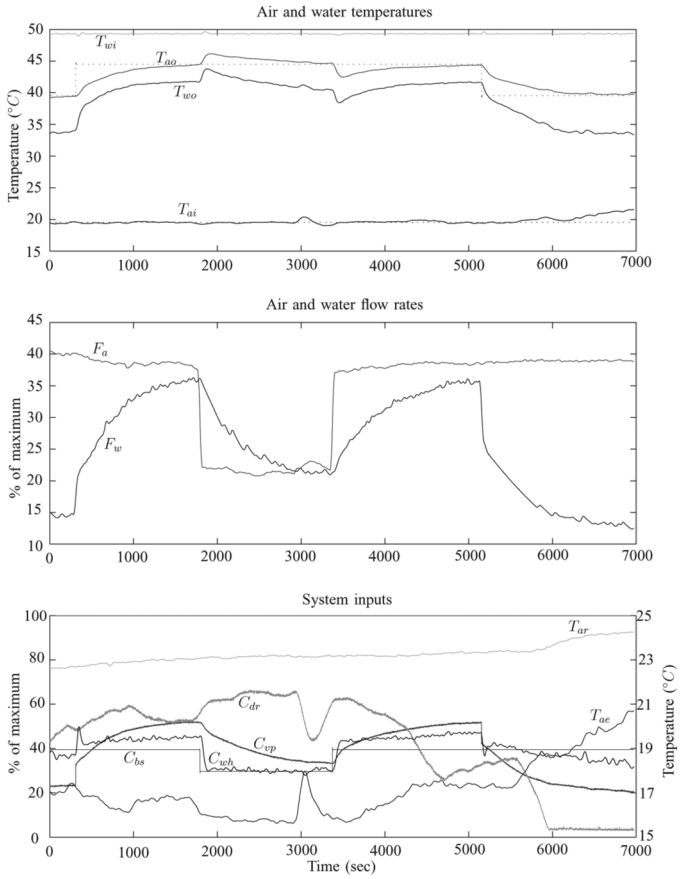

Fig. 6. Controller K_{PI} experimental test results.

command (C_{vp}) [decreasing the water flow rate (F_w)]. However, the output air temperature (T_{ao}) increased 1.65 °C before the water flow (F_w) was reduced and the temperature returned to the reference level (rT_{ao}) approximately 1400 s after initiation of the air flow rate change.

These experimental results demonstrate that an HVAC system is *not* an uncoupled dynamical system but rather a multivariable system. Specifically, this is illustrated by the inverse response from increasing the airflow rate (F_a) which decreased the output air temperature (T_{ao}). To the controller $K_{PI}^{T_{ao}}$ is a disturbance, and it is well known that PI controllers are good at disturbance rejection. Therefore, well-tuned PI controllers are able to provide acceptable performance in commercial applications. However, the overall performance is limited by the PI controllers inability to make coordinated control actions. Better performance may be achieved by using a multivariable controller that is able to make coordinated control actions. The Section VIII-B illustrates an example MIMO controller's ability to make coordinated control actions and the performance achieved as a result of coordinated control.

B. MIMO Robust Controller K_{R2} Verification

The controller setup in Fig. 5 was converted to a Simulink diagram (with RTW) that was used to test the performance of controller K_{R2}. Unlike the PI controller, this HVAC system was brought to steady state in open loop, and the loop was closed

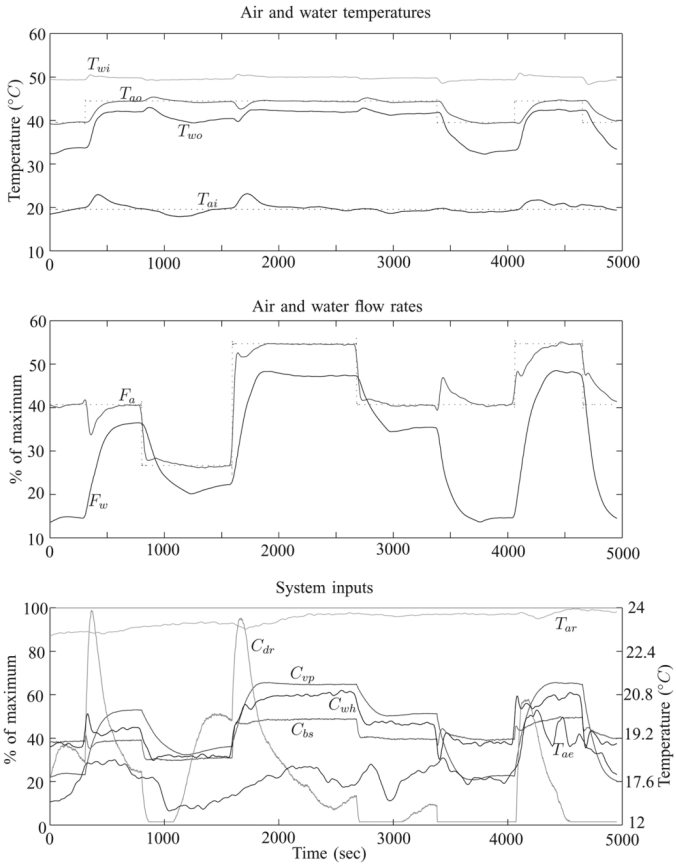

Fig. 7. Controller K_{R2} experimental test results.

using a (nearly) bumpless transfer technique. For details, see [1]. The closed-loop system (after the bumpless transfer had settled) was subjected to a series of step changes. The response of the experimental system to these inputs is shown in Fig. 7.

For an example step change, the output air temperature (rT_{ao}) reference was increased from 39.5 °C to 44.5 °C at around second 300. The controller responded by increasing both the valve position (C_{vp}) and water heater (C_{wh}) outputs, as well as (after first increasing) momentarily decreasing the blower speed output (C_{bs}) and briefly increasing the return air damper position output (C_{dr}). In response to these actions, the water flow rate (F_w) increased, the water supply temperature (T_{ws}) was maintained, the air flow rate (F_a) momentarily decreased and the input air temperature (T_{ai}) increased briefly. The output air temperature (T_{ao}) reached the specified temperature 322 s after the step in the reference signal. Since the controller K_{R2} controlled the input air temperature to in steady state, track a reference input (rT_{ai}), only momentary deviations were allowed. However, these momentary changes in input air temperature (T_{ai}) did aid in reducing the response time of the system.

For an example of disturbance rejection, the air flow rate reference (rF_a) was reduced from 0.29 m^3/s (40.7%) to 0.19 m^3/s (26.7%) at around second 800. The controller responded by rapidly reducing the blower speed output (C_{bs}) to 90%, then gradually to 100% 381 s after the step input. Simultaneously, while reducing the air flow rate (F_a), the controller momentarily reduced the return air damper (C_{dr}) output and reduced both the water heater (C_{wh}) and the valve position (C_{vp}) outputs. These actions momentarily lowered the input air temperature, maintained the water supply temperature and reduced the water flow rate (F_w).

For the MIMO controller, a step change in the reference output air temperature (rT_{ao}) occurred at the same time as an increase in the reference air flow rate (rF_a) (i.e., a disturbance in the presence of a step change) at around second 4000. The system responded by simultaneously increasing the blower speed (C_{bs}), valve position (C_{vp}), and water heater (C_{wh}) outputs while momentarily increasing the return air damper output (C_{dr}). These actions raised both the output air temperature (T_{ao}) and air flow rates (F_a) with the reference levels being reached in 304 and 387 s, respectively. These two actions would normally oppose each other, but the multivariable controller was able to simultaneously deal with both situations at once.

The coordinated control actions from this MIMO controller provided both a faster settling time and better disturbance rejection than the uncoupled PI controllers.

The MIMO controller presented here is only one possible controller architecture. Many different architectures are possible that build off of the design methodology used for the controller K_{R2}. This is demonstrated in Section IX where two other MIMO controller architectures are synthesized based on the system configuration in Fig. 3 and the weights designed in Section VII.

IX. Versatility of the Method

Many different controller architectures may be explored by redefining the vectors w_1, w_2, z_1, and z_2 (and in some cases u and y). For example, if you want to track a different signal, you would input the tracking error of the signal into the controller and define a performance weight for that controller input using a performance weight that is similar to the ones used in Section VII. As another example, if you want dynamic participation of one controlled signal while tracking another controlled signal, then the pole of the dynamically participating signal's performance weight could be moved to a lower frequency [1]. Examples of these types of modifications and their performance on the physical system are discussed in this section. The weights used in Section VII remain virtually unchanged for the alternative architectures studied here, since the model uncertainty weights were based on model inaccuracies (and unmodelled dynamics), and the optimization weights were based on the bandwidth of the components. Using these weights, two more MIMO robust controllers were created that had vastly different architectures. These controllers are labelled K_{R1} and K_{R3} and described next.

The MIMO controller K_{R1} was similar to K_{R2}, except it did not control the water supply. Instead, a separate PI controller was used to regulate the water temperature supplied to the DAS. This meant that the commanded water heater output (C_{wh}) was no longer included in the vectors z_2 and u, since it was controlled by the PI controller. Since the temperature of water out of the coil (T_{wo}) only affected the controller output C_{wh}, it was removed from the vector y, and the reference rT_{ws} was removed from the vector w_1, which resulted in a 6-input, 3-output MIMO robust controller.

TABLE VIII
COMPARISON OF CONTROLLER PERFORMANCE

Performance Measurement		Controller K_{PI}	K_{R1}	K_{R2}	K_{R3}	units
T_{ao}	Rise Time	891	150	178	91	sec.
	Settle Time	931	275	322	218	sec.
	Overshoot	0.0	2.8	2.0	4.0	%
	Disturbance Rejection	96.0	96.4	98.3	96.3	%
F_a	Rise Time	NA	199	42	44	sec.
	Settle Time	NA	214	46.7	51	sec.
	Overshoot	NA	1.1	1.5	2.0	%
	Disturbance Rejection	NA	77	83.6	88.7	%

The MIMO controller K_{R3} was a major shift from the current HVAC controller design paradigm. In this design, the temperature of water in the system (T_{ws}) was allowed to be varied for the individual DAS. In a building application, this would require individual water supplies for each zone to be regulated. In this design, the value of T_{ws} was given to the controller instead of $errorT_{ws}$ and the weights associated with $w_{\mathrm{Dist}}(rT_{ws})$ and $w_{\mathrm{Perf}}(T_{ws})$ were removed. For more information about the design of this controller and controller K_{R1}, see [1].

In terms of current HVAC controller architecture, individual K_{R1} controllers would be synthesized for each zone forming distributed control over the entire building. In contrast, controller K_{R2} would be designed as a central controller where the six measurements F_w, $errorFa$, $errorT_{ai}$, T_{wi}, T_{wo}, and $errorT_{ao}$ would come from each zone and the corresponding control signals C_{vp}, C_{bs}, and C_{dr} would be sent to control the zone, and the signals $errorT_{ws}$ and C_{wh} would be used to regulate the shared water supply. Finally, controller K_{R3} would be a distributed style controller that would be able to control each zone with its own water supply. The performance of these controller is compared in Section X.

X. PERFORMANCE OF DAS CONTROLLERS

Considering the architectural factors influencing the HVAC controller designs, the performance of the controllers on the experimental system are now contrasted. The settling times of the four DAS controllers in response to step changes in output air temperature and air flow rate are summarized in Table VIII. For each controller, the step in output air temperature was 5 °C (from 39.5 °C to 44.5 °C) and the step in flow rate of error was 0.1 m(^{3}/s) [from 0.29 (m^3/s) to 0.19 (m^3/s)]. These results demonstrate the potential performance increased that may be obtained from the coordinated actions of the MIMO controllers.

For a step change of 5 °C in the discharge air temperature, the system with the SISO PI controllers required 931 s to settle at the new level. This was 4.3 times longer than the time required by the fastest MIMO robust controller (K_{R3}) and 2.9 times longer than the slowest MIMO robust controller (K_{R2}). This suggests that a MIMO robust controller could achieve performance gains of 300% or more in tracking step changes. This capability could be used to heat specific parts of building only as they are needed and hence conserve energy. In fact, if we base the comfort of room by how fast the controller can hit 90% of its target (i.e., the rise time), the controller K_{R3} could have a room ready in 1.5 min, where the PI controller would take close to 15 min.

To simulate a disturbance, each of the controllers was subjected to a 0.12-m^3/s step change in air flow rate (rF_a) while trying to track an output air temperature (T_{ao}) of 44.5 °C. Disturbance rejection was measured in terms of how far the output air temperature varied in the presence of a disturbance (i.e., a 1.8 °C variation was 96% disturbance rejection). In the experiments ran, the MIMO robust controllers did slightly better at disturbance rejection than the PI controller.

From the preceding, controller K_{R3} clearly out-performed the other controllers. It also required independently controlled (separate) water supplies for each DAS being controlled and differed the most architecturally from today's systems.

XI. CONCLUSION

The experimental results demonstrate that the application of robust MIMO controls to an HVAC system offers a dramatic (more than 3 times) improvement in performance over current PI based HVAC controllers. Furthermore, increased performance may be realized without the increased cost associated with separate water supplies (for each DAS controlled), that are required with a "full MIMO" controller.

This brief was not intended to address the various PI designs (i.e., only a well tuned industry standard PI controller was used), but rather exemplify the design and implementation of MIMO robust controllers for various HVAC system architectures (one of which represents a major shift in the current design paradigm) and to demonstrate the improvement that would be expected on a commercial HVAC system. Other active areas in advance HVAC control include using reinforcement learning agents (and other adaptive control schemes) to improve the performance of a controller on the physical system, which were not addressed here. This article is based on the research in [1]) which was one of the first to approach HVAC controller design from a multivariable point of view.

REFERENCES

[1] M. L. Anderson, "MIMO robust control for heating, ventilating and air conditioning (HVAC) systems," M.S. thesis, Elect. Comput. Eng. Dept., Colorado State Univ., Fort Collins, 2001.

[2] M. L. Anderson, M. R. Buehner, P. M. Young, D. C. Hittle, C. W. Anderson, J. Tu, and D. Hodgson, "An experimental system for testing advanced heating, ventilating and air conditioning controllers," *Energy Buildings*, vol. 39, no. 2, pp. 136–147, Feb. 2007.

[3] J. B. Gary, C. D. John, G. Keith, P. Andy, and S. Roy, *μ-Analysis and Synthesis TOOLBOX User's Guide*. Natick, MA: Math Works, Inc., 1996, pp. 01760–1500.

[4] Y. H. Chen, K. M. Lee, and W. J. Wepfer, "Adaptive robust control scheme applied to a single-zone HVAC system," in *Proc. Amer. Control Conf.*, 1990, pp. 1076–1081.

[5] X. He, S. Liu, H. H. Asada, and H. Itoh, "Multivariable control of vapor compression systems," *Int. J. HVAC&R Res.*, vol. 4, no. 3, pp. 205–230, 1998.

[6] W. H. Roger and C. H. Douglas, *Control Systems for Heating, Ventilating, and Air Conditioning*, 5th ed. New York: Chapman & Hall, 1993.

[7] K. Masato, M. Tadahiko, H. Yukihiro, M. Itaru, K. Akiomi, K. Kazuyuki, and K. Shigeru, "Optimal preview control for HVAC system," in *Proc. ASHRAE Winter Meet.*, 1998, pp. 502–513.

[8] M. Kasahara, T. Matsuba, Y. Kuzuu, T. Yamazaki, Y. Hashimoto, K. Kamimura, and S. Kurosu, "Design and tuning of robust pid controller for HVAC systems," *ASHRAE Trans.*, vol. 105, no. 2, pp. 154–166, Jun. 1999.

[9] C. G. Nesler and W. F. Stoecker, "Selecting the proportional and integral constants in the direct digital control of discharge air temperature," *ASHRAE Trans.*, vol. 90, pp. 834–845, 1984.

[10] A. Packard and J. C. Doyle, "The complex structured singular value," *Automatica*, vol. 29, no. 1, pp. 71–109, 1993.
[11] G. Shaavit and S. G. Brandt, *The Dynamic Performance of a Discharge Air Temperature System With a P-I Controller*. Arlington Heights, IL: Honeywell Inc., Commercial Division, 1982.
[12] S. Sigurd and P. Ian, *Multivariable Feedback Control*. West Sussex, U.K.: Wiley, 1996.
[13] C. P. Underwood, "Robust control of HVAC plant II: Controller design," *Building Services Eng. Res. Technol.*, vol. 21, no. 1, pp. 63–71, 2000.
[14] S. W. Wang and X. H. Xu, "Optimal and robust control of outdoor ventilation airflow rate for improving energy efficiency and iaq," *Building Environment*, vol. 39, no. 7, pp. 763–773, 2004.
[15] P. M. Young, "Controller design with real parameteric uncertainty," *Int. J. Control*, vol. 65, pp. 469–509, 1996.
[16] M. Zaheer-Uddin, "Optimal, sub-optimal and adaptive control methods for the design of temperature controllers for intelligent buildings," *Building Environment*, vol. 28, no. 3, pp. 311–322, Jul. 1993.
[17] G. R. Zheng and M. Zaheer-Uddin, "Discharge air system: Modelling and optimal control," *Int. J. Energy Res.*, vol. 23, no. 8, pp. 727–738, Jun. 1999.